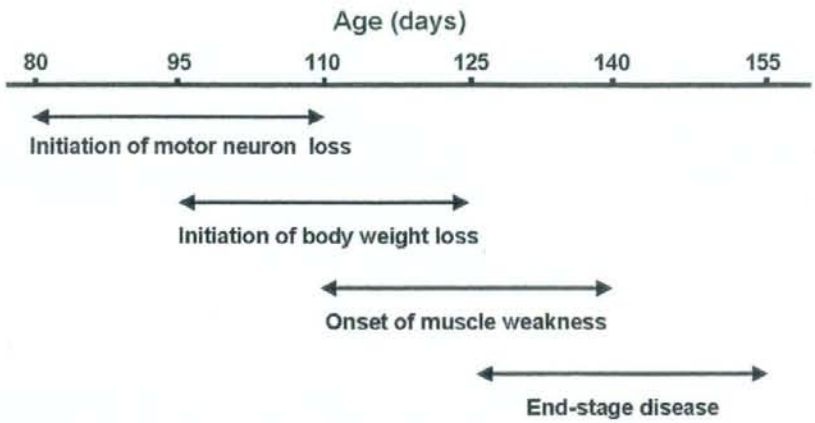


Fig. 8. Four stages of disease progression in hSOD1 (G93A) transgenic rats. The disease progression can be classified into four stages as shown. The range for each stage is about 1 month and overlaps approximately 2 weeks with the next stage.

O'Halloran, 2005), suggesting that the G93A mutation might accelerate the formation of SOD1 protein aggregates, which may ultimately sequester heat-shock proteins and molecular chaperones, disturb axonal transport or protein degradation machineries, including the ubiquitin-proteasome system (Borchelt et al., 1998; Bruening et al., 1999; Williamson and Cleveland 1999; Okado-Matsumoto and Fridovich 2002; Urushitani et al., 2002). Curiously, the mutated hSOD1 (G93A) protein is more susceptible to degradation by the ubiquitin-proteasome system and has a shorter half-life than other mutants (Fujiwara et al., 2005), suggesting that it may cause more unstable toxic aggregates in the spinal cord than other mutations. The degradation rate is also affected by environmental factors unique to each animal, such as the progressive decline of proteasome function with age (Keller et al., 2000), and these factors could contribute to the variability of the clinical course of G93A rats.

Taking all these findings into consideration, the mutated hSOD1 (G93A) protein may gain properties that are responsible for a variety of phenotypes and variability in the clinical course of the affected animals.

### Characteristics of Different Methods for Assessing hSOD1 (G93A) Transgenic Rats

The ideal measure is not influenced by the judgment of the observer, sensitive to small abnormalities, specific to detect pathologic events that are related to pathogenesis of the ALS-like disease, not influenced by the motivational factors of rats, minimal in the requirements for skill in the observer, and inexpensive to carry out. We assessed each evaluation method by the categories in regard to practical use as shown in the Table 6.

The initiation of body weight loss seems to be an excellent marker to detect the onset and should be highly recommended. Muscle volume might have already started to decrease, even in the period of continuous weight gain, as reported for hSOD1 (G93A) transgenic mice (Brooks et al., 2004). As a result, it could detect an abnormality relatively earlier than subjective onset. The inclined plane test is considered to be the least defective method of all. It could objectively and specifically detect the decline in the muscle strength of these ALS model rats as a muscle weakness onset almost at the same time of the subjective onset. The cage activity measurement and SCANET require very expensive apparatus, and are limited by the availability of funds and space for making the measurements. Although SCANET test was most sensitive among these measures, it seems inappropriate for the statistical analysis, and does not add any more information than that obtained through simple observation of the rats because the performances of the rats might be severely affected by the extent of their motivation to explore. Motor score can specifically assess disease progression of each clinical type and is valuable in keeping the experimental costs at a minimum.

### Correlation Between the Loss of Spinal Motor Neurons and Disease Stages

This study clearly shows the variable clinical course of G93A rats. According to our behavioral and histological analyses, we can divide the disease course of this transgenic model into four stages, whose durations have a range of about 1 month, as shown in Figure 8. Furthermore, we have established the pathological validity of the performance deficits detected by each measure of disease progression. "Initiation of motor neuron loss" was defined as a statistically significant decrease in the number of spinal motor neurons, which was found at around 90 days of age, but not 70 days of age (Fig. 7B). This coincides with, and seems to be sensitively detected by the marked difference in SCANET scores that begins at around 90 days of age (Fig. 3D–F). The "initiation of body weight loss" was usually detected at around 110 days of age as the peak body weight (pre-symptomatic onset, 113.6 ± 4.8 days of age, range = 103–124, Table IV). This stage coincides with the initiation of a rapid decline in the number of motor neurons at around 110 days of age (Fig. 7B). "Onset of muscle weakness" was detected at around 125 days of age, as assessed by the

inclined plane test (muscle weakness onset, 125.2 ± 7.4 days of age, range = 110–144, Table IV). This coincides with the number of spinal motor neurons in the transgenic rats being reduced to about 50% of the number in wild-type rats (Fig. 7B). We presume that transgenic rats do not present obvious muscle weakness until the number of motor neurons has been reduced to approximately half the number found in the healthy state. "End-stage disease" as defined by righting reflex failure was recorded at around 140 days of age (137.8 ± 7.1 days of age, range = 122–155, Table IV). At this stage, the affected rats had only about 25% of the spinal motor neurons of age- and gender-matched wild-type rats (Fig. 7B), and showed a generalized loss of motor activity. Thus, our findings allow us to estimate the extent of spinal motor neuron loss by evaluating the disease stage with the measures described in this study.

In summary, we have described the variable phenotypes of mutant hSOD1 (G93A) transgenic rats and established an evaluation system applicable to all clinical types of these rats. Disease stages defined by this evaluation system correlated well pathologically with the reduction of motor neurons. Our evaluation system of this animal model should be a valuable tool for future preclinical experiments aimed at developing novel treatments for ALS.

## ACKNOWLEDGMENTS

We thank Dr. H.-N. Dai of the Department of Neuroscience, Georgetown University School of Medicine for technical advice and valuable discussions, and Dr. T. Yoshizaki and Miss K. Kaneko for participating in the assessment of transgenic rats with the Motor score. This work was supported by grants from CREST, Japan Society for the Promotion of Science to H.O., a Research Grant on Measures for Intractable Diseases from the Japanese Ministry of Health, Labour and Welfare to H.O., M.A., G.S. and Y.I., and a Grant-in-Aid for the 21st century COE program to Keio University from the Japanese Ministry of Education, Culture, Sports, Science and Technology.

## REFERENCES

Abe K, Aoki M, Ikeda M, Watanabe M, Hirai S, Itoyama Y. 1996. Clinical characteristics of familial amyotrophic lateral sclerosis with Cu/Zn superoxide dismutase gene mutations. J Neurol Sci 136:108–116.

Azzouz M, Ralph GS, Storkebaum E, Walmsley LE, Mitrophanous KA, Kingsman SM, Carmeliet P, Mazarakis ND. 2004. VEGF delivery with retrogradely transported lentivector prolongs survival in a mouse ALS model. Nature 429:413–417.

Barneoud P, Lolivier J, Sanger DJ, Scatton B, Moser P. 1997. Quantitative motor assessment in FALS mice: a longitudinal study. Neuroreport 8:2861–2865.

Borchelt DR, Wong PC, Becher MW, Pardo CA, Lee MK, Xu ZS, Thinakaran G, Jenkins NA, Copeland NG, Sisodia SS, Cleveland DW, Price DL, Hoffman PN. 1998. Axonal transport of mutant superoxide dismutase 1 and focal axonal abnormalities in the proximal axons of transgenic mice. Neurobiol Dis 5:27–35.

Brooks KJ, Hill MD, Hockings PD, Reid DG. 2004. MRI detects early hindlimb muscle atrophy in Gly93Ala superoxide dismutase-1 (G93A SOD1) transgenic mice, an animal model of familial amyotrophic lateral sclerosis. NMR Biomed 17:28–32.

Brown RH Jr. 1995. Amyotrophic lateral sclerosis: recent insights from genetics and transgenic mice. Cell 80:687–692.

Bruening W, Roy J, Giasson B, Figlewicz DA, Mushynski WE, Durham HD. 1999. Up-regulation of protein chaperones preserves viability of cells expressing toxic Cu/Zn-superoxide dismutase mutants associated with amyotrophic lateral sclerosis. J Neurochem 72:693–699.

Chiu AY, Zhai P, Dal Canto MC, Peters TM, Kwon YW, Prattis SM, Gurney ME. 1995. Age-dependent penetrance of disease in a transgenic mouse model of familial amyotrophic lateral sclerosis. Mol Cell Neurosci 6:349–362.

de Belleroche J, Orrell R, King A. 1995. Familial amyotrophic lateral sclerosis/motor neurone disease (FALS): a review of current developments. J Med Genet 32:841–847.

Deng HX, Hentati A, Tainer JA, Iqbal Z, Cayabyab A, Hung WY, Getzoff ED, Hu P, Herzfeldt B, Roos RP, Warner C, Deng G, Soriano E, Smyth C, Parge HE, Ahmed A, Roses AD, Hallewell RA, Pericak-Vance MA, Siddique T. 1993. Amyotrophic lateral sclerosis and structural defects in Cu, Zn superoxide dismutase. Science 261:1047–1051.

Fujiwara N, Miyamoto Y, Ogasahara K, Takahashi M, Ikegami T, Takamiya R, Suzuki K, Taniguchi N. 2005. Different immunoreactivity against monoclonal antibodies between wild-type and mutant copper/zinc superoxide dismutase linked to amyotrophic lateral sclerosis. J Biol Chem 280:5061–5070.

Furukawa Y, O'Halloran TV. 2005. Amyotrophic lateral sclerosis mutations have the greatest destabilizing effect on the Apo- and reduced form of SOD1, leading to unfolding and oxidative aggregation. J Biol Chem 280:17266–17274.

Gale K, Kerasidis H, Wrathall JR. 1985. Spinal cord contusion in the rat: behavioral analysis of functional neurologic impairment. Exp Neurol 88:123–134.

Garbuzova-Davis S, Willing AE, Milliken M, Saporta S, Zigova T, Cahill DW, Sanberg PR. 2002. Positive effect of transplantation of hNT neurons (NTera 2/D1 cell-line) in a model of familial amyotrophic lateral sclerosis. Exp Neurol 174:169–180.

Gurney ME, Pu H, Chiu AY, Dal Canto MC, Polchow CY, Alexander DD, Caliendo J, Hentati A, Kwon YW, Deng HX, Chen W, Zhai F, Sufit RL, Siddique T. 1994. Motor neuron degeneration in mice that express a human Cu,Zn superoxide dismutase mutation. Science 264:1772–1775.

Hand CK, Rouleau GA. 2002. Familial amyotrophic lateral sclerosis. Muscle Nerve 25:135–159.

Howland DS, Liu J, She Y, Goad B, Maragakis NJ, Kim B, Erickson J, Kulik J, DeVito L, Psaltis G, DeGennaro LJ, Cleveland DW, Rothstein JD. 2002. Focal loss of the glutamate transporter EAAT2 in a transgenic rat model of SOD1 mutant-mediated amyotrophic lateral sclerosis (ALS). Proc Natl Acad Sci USA 99:1604–1609.

Inoue H, Tsukita K, Iwasato T, Suzuki Y, Tomioka M, Tateno M, Nagao M, Kawata A, Saido TC, Miura M, Misawa H, Itohara S, Takahashi R. 2003. The crucial role of caspase-9 in the disease progression of a transgenic ALS mouse model. EMBO J 22:6665–6674.

Kaspar BK, Llado J, Sherkat N, Rothstein JD, Gage FH. 2003. Retrograde viral delivery of IGF-1 prolongs survival in a mouse ALS model. Science 301:839–842.

Kato M, Aoki M, Ohta M, Nagai M, Ishizaki F, Nakamura S, Itoyama Y. 2001. Marked reduction of the Cu/Zn superoxide dismutase polypeptide in a case of familial amyotrophic lateral sclerosis with the homozygous mutation. Neurosci Lett 312:165–168.

Keller JN, Huang FF, Zhu H, Yu J, Ho YS, Kindy TS. 2000. Oxidative stress-associated impairment of proteasome activity during ischemia-reperfusion injury. J Cereb Blood Flow Metab 20:1467–1473.

Landis JR, Koch GG. 1977. The measurement of observer agreement for categorical data. Biometrics 33:159–174.

Mikami Y, Toda M, Watanabe M, Nakamura M, Toyama Y, Kawakami Y. 2002. A simple and reliable behavioral analysis of locomotor function after spinal cord injury in mice. Technical note. J Neurosurg Spine 97:142–147.

Mulder DW, Kurland LT, Offord KP, Beard CM. 1986. Familial adult motor neuron disease: amyotrophic lateral sclerosis. Neurology 36:511–517.

Nagai M, Aoki M, Miyoshi I, Kato M, Pasinelli P, Kasai N, Brown RH, Jr., Itoyama Y. 2001. Rats expressing human cytosolic copper-zinc superoxide dismutase transgenes with amyotrophic lateral sclerosis: associated mutations develop motor neuron disease. J Neurosci 21:9246–9254.

Ohki-Hamazaki H, Sakai Y, Kamata K, Ogura H, Okuyama S, Watase K, Yamada K, Wada K. 1999. Functional properties of two bombesin-like peptide receptors revealed by the analysis of mice lacking neuromedin B receptor. J Neurosci 19:948–954.

Okada Y, Shimazaki T, Sobue G, Okano H. 2004. Retinoic-acid-concentration-dependent acquisition of neural cell identity during in vitro differentiation of mouse embryonic stem cells. Dev Biol 275:124–142.

Okado-Matsumoto A, Fridovich I. 2002. Amyotrophic lateral sclerosis: a proposed mechanism. Proc Natl Acad Sci USA 99:9010–9014.

Ouary S, Bizat N, Altairac S, Menetrat H, Mittoux V, Conde F, Hantraye P, Brouillet E. 2000. Major strain differences in response to chronic systemic administration of the mitochondrial toxin 3-nitropropionic acid in rats: implications for neuroprotection studies. Neuroscience 97:521–530.

Rivlin AS, Tator CH. 1977. Objective clinical assessment of motor function after experimental spinal cord injury in the rat. J Neurosurg 47: 577–581.

Rosen DR, Siddique T, Patterson D, Figlewicz DA, Sapp P, Hentati A, Donaldson D, Goto J, O'Regan JP, Deng HX, Rahmani Z, Krizus A, McKenna-Yasek D, Cayabyab A, Gasten SM, Berger R, Tanzi RE, Halperin JJ, Herzfeldt B, van den Bergh R, Hung WY, Bird T, Deng G, Mulder DW, Smyth C, Laing NG, Soriano E, Pericak-Vance MA, Haines J, Reuleau GA, Gusella JS, Horvitz HR, Brown RH Jr. 1993. Mutations in Cu/Zn superoxide dismutase gene are associated with familial amyotrophic lateral sclerosis. Nature 362:59–62.

Shipp EL, Cantini F, Bertini I, Valentine JS, Banci L. 2003. Dynamic properties of the G93A mutant of copper-zinc superoxide dismutase as detected by NMR spectroscopy: implications for the pathology of familial amyotrophic lateral sclerosis. Biochemistry 42:1890–1899.

Storkebaum E, Lambrechts D, Dewerchin M, Moreno-Murciano MP, Appelmans S, Oh H, Van Damme P, Rutten B, Man WY, De Mol M, Wyns S, Manka D, Vermeulen K, Van Den Bosch L, Mertens N, Schmitz C, Robberecht W, Conway EM, Collen D, Moons L, Carmeliet P. 2005. Treatment of motoneuron degeneration by intracerebroventricular delivery of VEGF in a rat model of ALS. Nat Neurosci 8:85–92.

Sun W, Funakoshi H, Nakamura T. 2002. Overexpression of HGF retards disease progression and prolongs life span in a transgenic mouse model of ALS. J Neurosci 22:6537–6548.

Urushitani M, Kurisu J, Tsukita K, Takahashi R. 2002. Proteasomal inhibition by misfolded mutant superoxide dismutase 1 induces selective motor neuron death in familial amyotrophic lateral sclerosis. J Neurochem 83:1030–1042.

Wang LJ, Lu YY, Muramatsu S, Ikeguchi K, Fujimoto K, Okada T, Mizukami H, Matsushita T, Hanazono Y, Kume A, Nagatsu T, Ozawa K, Nakano I. 2002. Neuroprotective effects of glial cell line-derived neurotrophic factor mediated by an adeno-associated virus vector in a transgenic animal model of amyotrophic lateral sclerosis. J Neurosci 22: 6920–6928.

Watanabe M, Aoki M, Abe K, Shoji M, Iizuka T, Ikeda Y, Hirai S, Kurokawa K, Kato T, Sasaki H, Itoyama Y. 1997. A novel missense point mutation (S134N) of the Cu/Zn superoxide dismutase gene in a patient with familial motor neuron disease. Hum Mutat 9:69–71.

Weydt P, Hong SY, Kliot M, Moller T. 2003. Assessing disease onset and progression in the SOD1 mouse model of ALS. Neuroreport 14: 1051–1054.

Williamson TL, Cleveland DW. 1999. Slowing of axonal transport is a very early event in the toxicity of ALS-linked SOD1 mutants to motor neurons. Nat Neurosci 2:50–56.

J. Phys. Ther. Sci.
18: 33–41, 2006

# Hepatocyte Growth Factor in Mouse Soleus Muscle Increases with Reloading after Unloading

SHOJI TANAKA[1], KATSUHIKO TACHINO[1], EI KAWAHARA[2], JUNJI TANAKA[2], HIROSHI FUNAKOSHI[3], TOSHIKAZU NAKAMURA[3]

[1]*Department of Impairment Study, Graduate Course of Rehabilitation Science, Division of Health Sciences, Graduate School of Medical Science, Kanazawa University: 5-11-80 Kodatsuno, Kanazawa City, Ishikawa 920-0942, Japan. TEL +81 76-265-2500 E-mail: tanakas@mhs.mp.kanazawa-u.ac.jp*

[2]*Department of Clinical Laboratory Science, Graduate Course of Medical Science and Technology, Division of Health Sciences, Graduate School of Medical Science, Kanazawa University*

[3]*Division of Molecular Regenerative Medicine, Course of Advanced Medicine, Osaka University Graduate School of Medicine*

**Abstract.** Hepatocyte growth factor (HGF) has been suggested as a mitogen for skeletal muscle satellite cells and participates in skeletal muscle hypertrophy. The present study assessed HGF levels in mouse soleus and plantaris muscles during 14 days of tail suspension and 3 days of reloading using the enzyme-linked immunosorbent assay. Immunohistochemical analyses were used to determine the locations of HGF, its receptor (c-Met) and proliferating cell nuclear antigen. In normal mice, HGF contents were 4.4 ± 0.5 ng/g tissue in the soleus muscle and 5.9 ± 1.2 ng/g tissue in the plantaris muscle, significantly higher than in the soleus muscle. HGF level in the soleus muscle was increased 314% from normal by reloading. HGF and c-Met were expressed in small cells contiguous to muscle fibers. Cells in similar positions displayed reactivity for PCNA, suggesting that these represent activated satellite cells. Thus, production of HGF protein appears to stimulated in satellite cells during recovery from disuse atrophy.

**Key words:** Skeletal muscle atrophy, Satellite cell, Recovery

*(This article was submitted Oct. 17, 2005, and was accepted Dec. 8, 2005)*

## INTRODUCTION

Decreases in muscle activity due to spaceflight[1], unloading[2] and fixation of joints[3] often cause skeletal muscle atrophy. This is associated with a loss of contractile protein content due to decreases in overall protein synthesis[4] and increases in proteolysis[5]. Skeletal muscles have the ability to recover, from atrophy and increases in the activity of atrophied muscles result in hypertrophy and improvement of contractile function. Work-induced skeletal muscle hypertrophy is involved not only in the growth of muscle fiber size[6], but also in an increase in the number of myonuclei[7, 8].

Allen et al.[9] reported that the changes following atrophy or hypertrophy are not due to changes in the ratio of the myonuclear domain size to the amount of cytoplasm per myonucleus. Instead, skeletal muscle satellite cells play important roles in dramatic changes to myonuclei during hypertrophy. Satellite cells are mononucleated myogenic cells[10] that are generally found between the sarcolemma and

basement membrane. These cells usually remain in a resting or quiescent state[11] and are activated in response to mechanical stimulation[7, 8, 12] or muscle injury[13, 14].

Previous studies have suggested that the proliferation of satellite cells is stimulated by growth factors such as hepatocyte growth factor (HGF)[15, 16], insulin-like growth factors[17–19], fibroblast growth factors[20, 21], transforming growth factor $\beta$[10], platelet-derived growth factor BB[10, 14], and epidermal growth factor[17, 18]. However, only HGF has been shown to cause satellite cells to exit the $G_0$ phase and enter the $G_1$ phase in vitro[22, 23]. HGF was originally identified as a potent mitogen for hepatocytes[24], and has previously been reported to be expressed in various organs, including the liver, lungs, kidneys, thymus and spleen[25], and skeletal muscles[15, 16]. The complete amino-acid sequence of human HGF was reported in 1989[26]. HGF binds to the receptor c-Met[27], and activates cells expressing c-Met[28]. This receptor is a transmembrane tyrosine kinase that mediates the mitogenic signal for HGF[29, 30].

Although some studies have examined the role of HGF during maturation and regeneration of skeletal muscle, few attempts have been made to examine changes in HGF expression in hypertrophied and atrophied muscle in vivo. Only the content of HGF mRNA expression following denervation and compensatory overload[31], and of HGF protein following skeletal muscle injury[32], have been reported. These reports did not examine changes in HGF protein content following changes in muscle activities. The present study investigated changes in the morphology of skeletal muscles, expression of HGF protein, and locations of HGF, c-Met and proliferating cell nuclear antigen (PCNA) during unloading and subsequent reloading in the tail suspension model of hindlimb atrophy in mice.

## MATERIALS AND METHODS

*Animals and experimental design*

C57BL/6NCrj mice (8-weeks-old; initial body weight 17–19 g; Charles River Japan, Shizuoka, Japan) were used in this study. Mice were housed in a temperature-controlled room (20–24°C) with a 12-h light/12-h dark cycle and ad libitum access to laboratory chow and water. After 1 week, mice were randomly allocated to one of 3 groups: 2 experimental groups (Unloaded and Reloaded) and a control group (Control). Animals in the experimental groups were placed in individual cages and bilateral hindlimbs were unloaded for 14 days using Morey's tail suspension model[33]. After unloading, one of the 2 experimental groups underwent restoration of weight-bearing (reloading) for 3 days in standard cages. At the end of experimental period, all mice were anesthetized using diethyl ether, and their body weights were measured. Then, bilateral soleus and plantaris muscles of the hindlimbs were removed and immediately weighed using a digital analytical balance (Mettler Toledo, Tokyo, Japan), after which the mice were sacrificed. Ratios of muscle wet weight to body weight were used as the index of muscle change.

For histochemical analysis and immunofluorescence, one sample of each muscle was placed in Tissue-Tek Optimal Cutting Temperature compound (Miles, Elkhart, IN, USA), quick-frozen in liquid nitrogen-cooled isopentane, and stored at −70°C until use. Some muscle samples were fixed overnight in 10% formalin and then embedded in paraffin. Sections were then stained using hematoxylin and eosin (HE) for observation of histological features. Other muscle samples for measurement of HGF protein levels were chilled in liquid nitrogen. All procedures for animal care and treatment were performed in accordance with the *Guidelines for the Care and Use of Laboratory Animals* issued by Kanazawa University, and all protocols were approved by the IACUC of Kanazawa University.

*Enzyme-linked immunosorbent assay (ELISA) for HGF*

Muscle samples removed from bilateral hindlimbs were homogenized in rat HGF organic extraction buffer containing 20 mM Tris-HCl, 2 M NaCl, 0.1% Tween 80 and 1 mM phenylmethylsulfonyl fluoride (3 animals/sample). HGF levels in solution were measured using the rat HGF ELISA system (Institute of Immunology, Tokyo, Japan).

*Histological and immunohistochemical analysis*

To determine the ratio of type II fibers to total muscle fibers and to perform immunofluorescence for HGF, 8- and 6-$\mu$m frozen sections were cut using a cryostat (Sakura Finetek, Tokyo, Japan) cooled to −20°C, then dried for 2 h at room

temperature. Type I and II fibers in transverse sections (8 μm thick) were stained for myosin ATPase at pH 10.7. Lightly and darkly stained muscle fibers were classified as type I and II fibers, respectively. More than 150 randomly selected muscle fibers were measured per muscle section, and the percentage of type II fibers among the total number of fibers was calculated.

*Immunofluorescence*

Frozen transverse sections (6 μm thick) were fixed in methanol for 5 min at 4°C, then treated with 0.1% Triton X-100 in phosphate buffered saline (PBS) for 5 min. Non-specific binding sites were blocked using 10% normal swine serum and 1% bovine serum albumin (BSA) in PBS for 30 min. Sections were incubated with 1:10 polyclonal anti-rat HGF antibody (Institute of Immunology) in PBS or 1:40 normal rabbit serum (negative control) for 2 h at 37°C, followed by 1:600 goat anti-rabbit Alexa Fluor 488 (Molecular Probes, Eugene, OR, USA) in PBS for 20 min at room temperature. All nuclei were counterstained using 4',6-diamidino-2-phenylindole dihydrochloride (Molecular Probes). Sections were mounted in Gel/Mount (Cosmo Bio, Tokyo, Japan). Fluorescein signals in sections were observed and photographed under a fluorescence microscope (Olympus, Tokyo, Japan).

*Immunoperoxidase*

Tissues embedded in paraffin were cut 4 μm thick, placed on silane-coated slides, dewaxed with xylene, and dehydrated in ethanol. Endogenous peroxidases were blocked by incubation in 3% hydrogen peroxide for 10 min. Non-specific binding sites were blocked for 15 min with PBS containing 10% normal swine serum and 1% BSA. For HGF, sections were incubated overnight at 4°C with 1:500 anti-rat HGF antibody (Institute of Immunology) in PBS containing 10% normal swine serum and 1% BSA, then HGF was detected using the CSA System (Dako Cytomation Japan, Kyoto, Japan) in accordance with the instructions provided by the manufacturer. For c-Met, sections were incubated overnight at 4°C with 1 μg/ml rabbit polyclonal anti-c-Met antibody (Santa Cruz Biotechnology, Santa Cruz, CA, USA). Sections were incubated for 60 min at room temperature with horseradish peroxidase-labeled polymer conjugated with goat anti-rabbit immunoglobulin (Dako Cytomation Japan). Antigenic sites were visualized with 3',3-diaminobenzidine tetrahydrochloride using a commercial kit (Dako Cytomation Japan) and then counterstained with hematoxylin.

For immunohistochemical staining of PCNA, sections were incubated with mouse monoclonal anti-PCNA antibody (ready-to-use, clone PC10; Dako Cytomation Japan) or normal mouse serum (negative control, ready-to-use; Dako Cytomation Japan), followed by 60 min incubation at room temperature with horseradish peroxidase-labeled polymer conjugated with goat anti-mouse immunoglobulin. Immunoreactive protein was visualized using 3',3-diaminobenzidine tetrahydrochloride (Dako Cytomation Japan). Nuclei were counterstained using hematoxylin. As a negative control, normal rabbit serum or normal mouse serum was used instead of primary antibodies (Dako Cytomation Japan).

*Statistical analyses*

Data are presented as means ± standard deviation (SD). Differences between soleus and plantaris muscles were assessed using Student's or Welch's *t*-test. Differences between groups were detected by one-way analysis of variance (ANOVA) followed by Scheffe's post hoc test. For all tests, values of $P<0.05$ were considered statistically significant.

## RESULTS

*Damage to muscles*

Muscle wet weights and body weights were measured and the ratio calculated. Ratios were significantly lower in unloaded soleus and plantaris muscles than in control muscles, and reloading restored the ratios to normal levels (Table 1).

To determine the morphological effects of unloading and reloading, transverse sections of soleus and plantaris muscles were examined under an optical microscope. After loss of loading for 14 days, plantaris muscles showed atrophy and derangement of fiber alignment. No clear degeneration of muscle fibers was apparent (Fig. 1B, E). However, degeneration in the soleus muscle resulted in infiltration of macrophages and a marked presence of fibers displaying central nuclei after reloading (Fig. 1C). Furthermore, the number of nuclei in reloaded soleus muscles was increased, indicating regeneration (Fig. 1C). Degeneration and regeneration were not clearly observed in the

**Table 1.** Body weight and muscle mass in soleus and plantaris muscles

| | Soleus muscle | | | Plantaris muscle | | |
|---|---|---|---|---|---|---|
| | Control (n=20) | Unloaded (n=20) | Reloaded (n=20) | Control (n=20) | Unloaded (n=20) | Reloaded (n=20) |
| Muscle wet wt (mg) | 15.0 ± 1.1 | 9.8 ± 1.2* | 13.6 ± 1.6 | 27.7 ± 1.9 | 24.9 ± 1.8* | 27.6 ± 1.7 |
| Body wt (g) | 20.8 ± 0.7 | 20.5 ± 1.1 | 20.1 ± 1.1 | 20.8 ± 0.7 | 20.5 ± 1.1 | 20.1 ± 1.1 |
| Muscle wet wt/ body wt (mg/g) | 0.72 ± 0.04 | 0.48 ± 0.07* | 0.68 ± 0.08 | 1.33 ± 0.04 | 1.21 ± 0.07* | 1.38 ± 0.08 |

Values expressed as mean ± SD. * = Significantly different ($P<0.05$) from control and reloaded. Wt = weight.

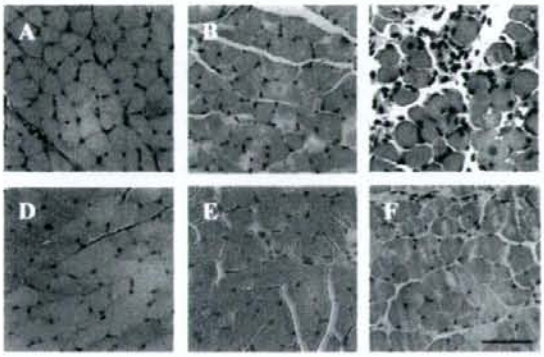


**Fig. 1.** HE staining of cross-sections from mouse soleus and plantaris muscles. Normal soleus muscle (A) and plantaris muscle (D); soleus muscle (B) and plantaris muscle (E) following 14 days of unloading; soleus muscle (C) and plantaris muscle (F) following 14 days of unloading followed by 3 days of reloading. Derangement of muscle fiber alignment is apparent following unloading (B, E) and reloading (C, F). Soleus muscle shows infiltration of macrophages, fibers with central nuclei and an increase in myogenetic nuclei (C) following 14 days of unloading followed by 3 days of reloading. Scale bar, 50 $\mu$m.

plantaris muscle (Fig. 1F).

Staining for muscle myosin ATPase clearly distinguished lightly stained type I fibers from darker type II fibers (Fig. 2). Type II fibers were dominant in the soleus muscle, while type I fibers were dominant in the plantaris muscle (Table 2). The ratio of type II fibers to total fibers did not differ significantly between groups (Table 2).

*Changes in HGF level*

HGF levels in mouse skeletal muscles were quantified using ELISA. In normal mice, HGF contents were 4.4 ± 0.5 ng/g tissue in the soleus muscle and 5.9 ± 1.2 ng/g tissue in the plantaris muscle. Soleus and plantaris muscles unloaded for 14 days tended to display slightly reduced HGF levels, but no significant difference was identified. Reloading for 3 days after 14-day unloading significantly increased HGF levels in the soleus muscle (Table 3). According to ELISA results, reloading after unloading resulted in a 314% increase in the level of HGF protein in soleus muscles as compared to control soleus muscles. The HGF level was significantly higher in reloaded soleus muscles than in control or unloaded soleus muscles. In contrast, the HGF level in plantaris muscles was not significantly changed after reloading. The HGF level was significantly lower

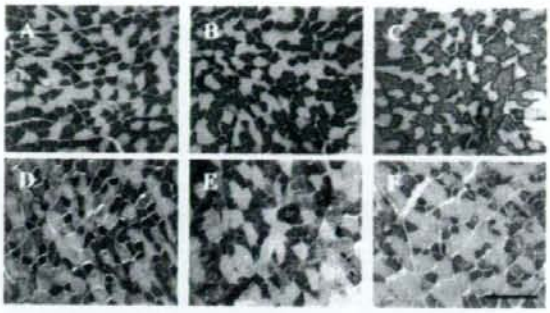

**Fig. 2.** Myosin ATPase staining of cross-sections from mouse soleus and plantaris muscles. Normal soleus muscle (A) and plantaris muscle (D); soleus muscle (B) and plantaris muscle (E) following 14 days of unloading; soleus muscle (C) and plantaris muscle (F) following 14 days of unloading followed by 3 days of reloading. Type I fibers stain lightly, while type II fibers stain dark. Scale bar, 100 $\mu$m.

**Table 2.** Proportion of type II fibers total muscle fibers (%)

| | Soleus muscle | Plantaris muscle |
|---|---|---|
| Control | 69.5 ± 1.9 | 43.2 ± 4.5 |
| Unloaded | 71.9 ± 4.6 | 52.8 ± 9.8 |
| Reloaded | 70.6 ± 3.4 | 45.2 ± 3.7 |

Results represent means ± SD (n=5).

**Table 3.** HGF protein concentrations in mice soleus and plantaris muscles

| | HGF protein concentration (ng/g tissue) | |
|---|---|---|
| | Soleus muscle | Plantaris muscle |
| Control | 4.4 ± 0.5[c] | 5.9 ± 1.2 |
| Unloaded | 3.2 ± 1.6 | 4.3 ± 1.2 |
| Reloaded | 13.8 ± 5.0[abc] | 6.5 ± 1.4 |

Results represent means ± SD (n=5). [a]$P<0.05$ vs. controls; [b]$P<0.05$ vs. unloaded; [c]$P<0.05$ vs. plantaris muscle.

in control soleus muscles than in control plantaris muscles, but it was significantly higher in reloaded soleus muscles than in reloaded plantaris muscles.

*Immunolocalization of HGF, c-Met and PCNA*

Localization of HGF was determined by immunoperoxidase using formalin-fixed and paraffin-embedded tissues and immunofluorescence using unfixed frozen tissues. HGF was observed in the cytoplasm of satellite cells, which were seen as small cells contiguous with and distinct to muscle fibers in paraffin sections of reloaded soleus muscle (Fig. 3A, B). No HGF was identified in control or unloaded soleus muscle. Plantaris muscles in all conditions were negative for HGF immunostaining. Immunofluorescence in frozen sections of reloaded soleus muscles also showed positive results for HGF around nuclei in the small satellite cells adjacent to large muscle cells (Fig. 3D, E). Negative control sections stained with normal rabbit serum instead of anti-HGF antibodies did not display any specific signals for HGF (Fig. 3C, F). In addition, c-Met was identified in the small satellite cells in the membrane facing adjacent muscle cells (Fig. 4A). To distinguish small satellite cells from quiescent muscle fiber cells and infrequently dividing macrophages, cell division ability was assessed using PCNA histochemistry, which generally stains/visualizes the $G_1$ or S phase of the cell cycle. PCNA-positive cells were present alongside muscle fibers and were considered to represent cells similar to HGF- and c-Met-positive cells (Fig. 4C).

## DISCUSSION

In our experiments, quantitative and morphological atrophy of the soleus and plantaris muscles was caused by unloading for 14 days. Supporting the current findings, a previous study[34]

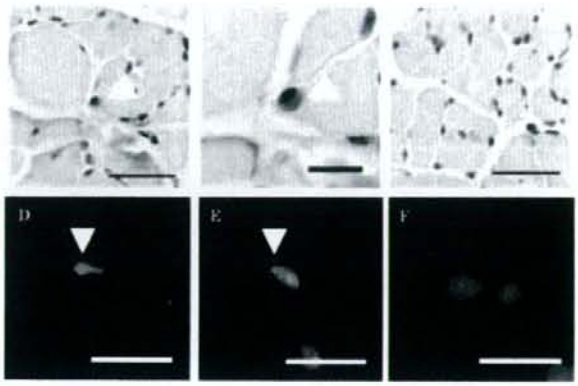


**Fig. 3.** HGF immunolocalization in reloaded soleus muscle. The upper row (A–C) shows immunoperoxidase. Arrows indicate HGF in the cytoplasm of small cells contiguous to muscle fibers (A, B). The lower row (D–F) shows immunofluorescence. E and F: nuclei (blue) are observed surrounding muscle fibers. D and E: HGF (green) is localized in satellite cells surrounding adjacent muscle fibers (arrows). Negative controls stained using normal rabbit serum did not display positive results for HGF (C, F). Scale bar, 30 $\mu$m in A and C, 10 $\mu$m in B and 20 $\mu$m in D–F.

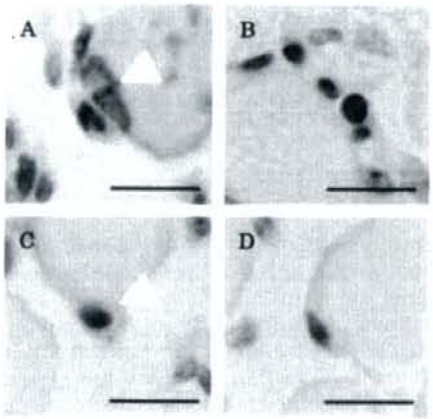


**Fig. 4.** Immunohistochemical localization for c-Met and PCNA in reloaded soleus muscle. Positive results for c-Met are apparent in small cells contiguous with muscle fibers (arrow). Myogenic nuclei (A) in a similar position display positive reactivity to PCNA, suggesting that these cells represent activated satellite cells (arrow). PCNA-positive cells (C) are present along with mononuclear cells. Negative controls stained using normal rabbit serum or normal mouse serum did not display positive results for c-Met or PCNA (B, D). Scale bar, 10 $\mu$m.

found that the mass of both soleus and plantaris muscles in rats decreased following hindlimb suspension for 2 weeks. Atrophy might be caused by myonuclear cell apoptosis[9, 35, 36], reduced protein synthesis[4] or activation of proteolytic systems such as the ubiquitin-proteasome system[37, 38], calpain system[39] and cathepsin D system[5]. The masses of both muscles normalized after 3 days of reloading following the 2 weeks of unloading. Thus, both soleus and plantaris muscles are able to recover following atrophy. However, the process leading to recovery seems to differ, with degeneration and regeneration occurring in the recovery process in the soleus muscle, but not in the plantaris muscle. Previous studies have reported that numbers of myonuclear cells per unit area increase following reloading of atrophied soleus muscle[8, 9, 40, 41] and this was also observed in the present study. The soleus muscle is known as an antigravity muscle containing slow-twitch fibers. ATPase staining shows that proportions of muscle fiber types differ between the soleus and plantaris muscles. Analysis of myosin heavy chain (MHC) isoforms has likewise indicated a difference, showing 40–70% MHC type I in mouse soleus muscle corresponding to type I fibers[42, 43], while mouse plantaris muscle contains predominantly type IIa and IIB MHCs

corresponding to type II fibers[44]. Electromyography shows that muscle activity in the rat soleus muscle increases during treadmill locomotion after hindlimb unloading[45]. Although the precise mechanisms are unknown, differing processes may be related to these differences in muscle fiber types. In addition, satellite cells are central to regeneration and could explain how these differences contribute to the process of degeneration and regeneration. Previous studies have reported that satellite cells comprise approximately 2% of the myonuclear population in the tibialis anterior muscle of 4-month-old mice and 9.6% in the soleus muscle of 1-month-old rats[11, 46]. Furthermore, mitotic activity of satellite cells in the soleus muscle is 0.052% in 24-month-old rats[47]. These findings show that slow muscles display a higher number of satellite cells than other muscles.

Reloading increased the level of HGF in the soleus muscle by approximately 3-fold compared to controls. This agrees with a previous report that HGF levels in rat quadriceps muscles increase in response to muscle injury[32]. Patterns of local injury, such as infiltration of macrophages and degeneration of muscle fibers and central nuclear cells, were observed following reloading of the soleus muscle. We also found that the HGF appears to be present in satellite cells surrounding uninjured small muscle fibers. Previous studies have reported that HGF is present in the extracellular matrix surrounding muscle fibers[16, 48], or immunolocalized at regenerating skeletal muscle[49]. In situ hybridization has also revealed HGF mRNA in regenerating muscle fibers[15, 31]. In the present study, HGF was clearly immunolocalized in the cytoplasm of satellite cells early in the recovery process, strongly suggesting that HGF is produced by local satellite cells in response to reloading stimulation. Muscle fiber injury induces macrophage infiltration, but HGF mRNA is not present in macrophages, as demonstrated by Jennische et al.[15] and the present study. Furthermore, c-Met was expressed in the cell membranes of satellite cells. Satellite cells display c-Met in all states of activation, proliferation and differentiation[27] and c-Met can be used as a molecular marker for these cells. The satellite cell is known as a quiescent muscle progenitor cell, and injury leads to cell activation[50]. After reloading, the majority of satellite cells were PCNA-positive, indicating that cells had entered the cell cycle. HGF- and HGF-receptor-positive cells are thus activated satellite cells. Taken together, recovery appears to be partially accomplished by proliferation and maturation of satellite cells, and proliferation of satellite cells seems likely to occur in an autocrine or paracrine manner with satellite cells producing HGF, followed by HGF activating the HGF-receptor-positive cells, satellite cells.

In conclusion, these results suggest that HGF production, stimulated in satellite cells, is the cause of recovery following mechanical stimulation in disuse-atrophied muscle.

## ACKNOWLEDGEMENTS

We would like to thank Prof. Toshio Nakatani from the Division of Health Sciences, Graduate School of Medical Science, Kanazawa University for supporting the present study.

## REFERENCES

1) Widrick JJ, Romatowski JG, Norenberg KM, et al.: Functional properties of slow and fast gastrocnemius muscle fibers after a 17-day spaceflight. J Appl Physiol, 2001, 90: 2203–2211.
2) Booth FW, Gollnick PD: Effects of disuse on the structure and function of skeletal muscle. Med Sci Sports Exerc, 1983, 15: 415–420.
3) Eichelberger L, Roma M, Moulder PV: Effects of immobilization atrophy on the histochemical characterization of skeletal muscle. J Appl Physiol, 1958, 12: 42–50.
4) Howard G, Steffen JM, Geoghegan TE: Transcriptional regulation of decreased protein synthesis during skeletal muscle unloading. J Appl Physiol, 1989, 66: 1093–1098.
5) Taillandier D, Aurousseau E, Combaret L, et al.: Regulation of proteolysis during reloading of the unweighted soleus muscle. Int J Biochem Cell Biol, 2003, 35: 665–675.
6) Mozdziak PE, Pulvermacher PM, Schultz E: Muscle regeneration during hindlimb unloading results in a reduction in muscle size after reloading. J Appl Physiol, 2001, 91: 183–190.
7) Rosenblatt JD, Yong D, Parry D: Satellite cell activity is required for hypertrophy of overloaded adult rat muscle. Muscle Nerve, 1994, 17: 608–613.
8) Smith HK, Maxwell L, Rodfers CD, et al.: Exercise-enhanced satellite cell proliferation and new myonuclear accretion in rat skeletal muscle. J Appl Physiol, 2001, 90: 1407–1414.
9) Allen DL, Roy RR, Edgerton VR: Myonuclear domains in muscle adaptation and disease. Muscle Nerve, 1999, 22: 1350–1360.

10) Mauro A: Satellite cells of skeletal muscle fibers. J Cell Biol, 1961, 9: 493–495.
11) Schultz E, Gibson MC, Champion T: Satellite cells are mitotically quiescent in mature mouse muscle: an EM and radioautographic study (1). J Exp Zool, 1978, 206: 451–456.
12) Darr KC, Schultz E: Exercise-induced satellite cell activation in growing and mature skeletal muscle. J Appl Physiol, 1987, 63: 1816–1821.
13) Bischoff R: A satellite cell mitogen from crushed adult muscle. Dev Biol, 1986, 115: 140–147.
14) Snow MH: Myogenic cell formation in regenerating rat skeletal muscle injured by mincing, II. An autoradiographic study. Anat Rec, 1997, 188: 201–218.
15) Jennische E, Ekberg S, Matejka GJ: Expression of hepatocyte growth factor in growing and regenerating rat skeletal muscle. Am J Physiol Cell Physiol, 1993, 265: C122–C128.
16) Tatsumi R, Anderson JE, Nevoret CJ, et al.: HGF/SF is present in normal adult skeletal muscle and is capable of activating satellite cells. Dev Biol, 1998, 194: 114–128.
17) Cook DR, Doumit ME, Merkel RA: Transforming growth factor-beta, basic fibroblast growth factor, and platelet-derived growth factor-BB interact to affect proliferation of clonally derived porcine satellite cells. J Cell Physiol, 1993, 157: 307–312.
18) Doumit ME, Cook DR, Merkel RA: Fibroblast growth factor, epidermal growth factor, insulin-like growth factors, and platelet-derived growth factor-BB stimulate proliferation of clonally derived porcine myogenic satellite cells. J Cell Physiol, 1993, 157: 326–332.
19) Phelan JN, Gonyea WJ: Effect of radiation on satellite cell activity and protein expression in overloaded mammalian skeletal muscle. Anat Rec, 1997, 247: 179–188.
20) Kastner S, Elias MC, Rivera AJ, et al.: Gene expression patterns of the fibroblast growth factors and their receptors during myogenesis of rat satellite cells. J Histochem Cytochem, 2000, 48: 1079–1096.
21) Yablonka-Reuveni Z, Seger R, Rivera AJ: Fibroblast growth factor promotes recruitment of skeletal muscle satellite cells in young and old rats. J Histochem Cytochem, 1999, 47: 23–42.
22) Allen RE, Sheehan SM, Taylor RG, et al.: Hepatocyte growth factor activates quiescent skeletal muscle satellite cells in vitro. J Cell Physiol, 1995, 165: 307–312.
23) Wozniak AC, Kong J, Bock E, et al.: Signaling satellite-cell activation in skeletal muscle: markers, models, stretch, and potential alternate pathways. Muscle Nerve, 2005, 31: 283–300.
24) Nakamura T, Nawa K, Ichihara A: Partial purification and characterization of hepatocyte growth factor from serum of hepatectomized rats. Biochem Biophys Res Commun, 1984, 122: 1450–1459.
25) Tashiro K, Hagiya M, Nishizawa T, et al.: Deduced primary structure of rat hepatocyte growth factor and expression of the mRNA in rat tissues. Proc Natl Acad Sci U S A, 1990, 87: 3200–3204.
26) Nakamura T, Nishizawa T, Hagiya M, et al.: Molecular cloning and expression of human hepatocyte growth factor. Nature, 1989, 342: 440–443.
27) Cornelison DDW, Wold B: Single-cell analysis of regulatory gene expression in quiescent and activated mouse skeletal muscle satellite cells. Dev Biol, 1997, 191: 270–283.
28) Sheehan SM, Tatsumi R, Temm-Grove JJ: HGF is an autocrine growth factor for skeletal muscle satellite cells in vitro. Muscle Nerve, 2000, 23: 239–245.
29) Bottaro DP, Rubin JS, Faletto DL, et al.: Identification of the hepatocyte growth factor receptor as the c-met proto-oncogene product. Science, 1991, 251: 802–804.
30) Ferracini R, Longati P, Naldini L, et al.: Identification of the major autophosphorylation site of the Met/hepatocyte growth factor receptor tyrosine kinase. J Biol Chem, 1991, 266: 19558–19564.
31) Yamaguchi A, Ishii H, Morita I, et al.: mRNA expression of fibroblast growth factors and hepatocyte growth factor in rat plantaris muscle following denervation and compensatory overload. Pflugers Arch, 2004, 448: 539–546.
32) Suzuki S, Yamanouchi K, Soeta C, et al.: Skeletal muscle injury induces hepatocyte growth factor expression in spleen. Biochem Biophys Res Commun, 2002, 292: 709–714.
33) Morey-Holton ER, Globus RK: Hindlimb unloading rodent model: technical aspects. J Appl Physiol, 2002, 92: 1367–1377.
34) Diffee GM, Haddad F: Control of myosin heavy chain expression: interaction of hypothyroidism and hindlimb suspension. Am J Physiol Cell Physiol, 1991, 261: C1099–C1106.
35) Allen DL, Linderman JK, Roy RR, et al.: Apoptosis: a mechanism contributing to remodeling of skeletal muscle in response to hindlimb unweighting. Am J Physiol Cell Physiol, 1997, 273: C579–C587.
36) Siu PM, Pistilli EE, Butler DC, et al.: Aging influences cellular and molecular responses of apoptosis to skeletal muscle unloading. Am J Physiol Cell Physiol, 2005, 288: C338–C349.
37) Bodine SC, Latres E, Baumhueter S, et al.: Identification of ubiquitin ligases required for skeletal muscle atrophy. Science, 2001, 294: 1704–1708.
38) Price SR: Increased transcription of ubiquitin-proteasome system components: molecular responses associated with muscle atrophy. Int J Biochem Cell Biol, 2003, 35: 617–628.
39) Huang J, Forsberg NE: Role of calpain in skeletal-muscle protein degradation. Proc Natl Acad Sci U S A, 1998, 95: 12100–12105.
40) Nguyen HX, Tidball JG: Expression of a muscle-specific, nitric oxide synthase transgene prevents muscle membrane injury and reduces muscle

inflammation during modified muscle use in mice. J Physiol (Lond), 2003, 5502: 347–356.
41) Putman CT, Dusterhoft S, Pette D: Changes in satellite cell content and myosin isoforms in low-frequency-stimulated fast muscle of hypothyroid rat. J Appl Physiol, 1999, 86: 40–51.
42) Carlson CJ, Booth FW, Gordon SE: Skeletal muscle myostatin mRNA expression is fiber-type specific and increases during hindlimb unloading. Am J Physiol Regul Integr Comp Physiol, 1999, 277: R601–R606.
43) Jin T-E, Witzemann V, Brecht M: Fiber types of the intrinsic whisker muscle and whisking behavior. J Neurosci, 2004, 24: 3386–3393.
44) Miyazaki M, Hitomi Y, Kizaki T, et al.: Contribution of the calcineurin signaling pathway to overload-induced skeletal muscle fiber-type transition. J Physiol Pharmacol, 2004, 55: 751–764.
45) Canu MH, Falempin M: Effect of hindlimb unloading on two hindlimb muscles during treadmill locomotion in rats. Eur J Appl Physiol, 1997, 75: 283–288.
46) Gibson MC, Schultz E: Age-related differences in absolute numbers of skeletal muscle satellite cells. Muscle Nerve, 1983, 6: 574–580.
47) McCormick KM, Thomas DP: Exercise-induced satellite cell activation in senescent soleus muscle. J Appl Physiol, 1992, 72: 888–893.
48) Tatsumi R, Allen RE: Active hepatocyte growth factor is present in skeletal muscle extracellular matrix. Muscle Nerve, 2004, 30: 654–658.
49) Hayashi S, Aso H, Watanabe K, et al.: Sequence of IGF-I, IGF-II, and HGF expression in regenerating skeletal muscle. Histochem Cell Biol, 2004, 122: 427–434.
50) Grounds MD, White JD, Rosenthal N, et al.: The role of stem cells in skeletal and cardiac muscle repair. J Histochem Cytochem, 2002, 50: 589–610.

BRAIN RESEARCH 1111 (2006) 187–195

available at www.sciencedirect.com

ScienceDirect

www.elsevier.com/locate/brainres

BRAIN RESEARCH

Research Report

# Adenoviral gene transfer of hepatocyte growth factor prevents death of injured adult motoneurons after peripheral nerve avulsion

Yuichi Hayashi[a,b], Yoko Kawazoe[a], Tsuyoshi Sakamoto[a], Miyoko Ojima[a], Wei Wang[a], Takanori Takazawa[a], Daisuke Miyazawa[c], Wakana Ohya[c], Hiroshi Funakoshi[c], Toshikazu Nakamura[c], Kazuhiko Watabe[a,*]

[a]Department of Molecular Neuropathology, Tokyo Metropolitan Institute for Neuroscience, Tokyo Metropolitan Organization for Medical Research, 2-6 Musashidai, Fuchu, Tokyo 183-8526, Japan
[b]Department of Neurology and Geriatrics, Gifu University Graduate School of Medicine, 1-1 Yanagido, Gifu 501-1194, Japan
[c]Division of Molecular Regenerative Medicine, Department of Biochemistry and Molecular Biology, Osaka University Graduate School of Medicine, B-7, Suita, Osaka 565-0871, Japan

ARTICLE INFO

*Article history:*
Accepted 27 June 2006
Available online 1 August 2006

*Keywords:*
Adult rat
Avulsion
Facial nerve
Hepatocyte growth factor
Motoneuron
Spinal nerve

ABSTRACT

Hepatocyte growth factor (HGF) exhibits strong neurotrophic activities on motoneurons both in vitro and in vivo. We examined survival-promoting effects of an adenoviral vector encoding human HGF (AxCAhHGF) on injured adult rat motoneurons after peripheral nerve avulsion. The production of HGF in COS1 cells infected with AxCAhHGF and its bioactivity were confirmed by ELISA, Western blot and Madin-Darby canine kidney (MDCK) cell scatter assay. The facial nerve or the seventh cervical segment (C7) ventral and dorsal roots of 3-month-old Fischer 344 male rats were then avulsed and removed from the stylomastoid or vertebral foramen, respectively, and AxCAhHGF, AxCALacZ (adenovirus encoding β-galactosidase gene) or phosphate-buffered saline (PBS) was inoculated in the lesioned foramen. Treatment with AxCAhHGF after avulsion significantly prevented the loss of injured facial and C7 ventral motoneurons as compared to AxCALacZ or PBS treatment and ameliorated choline acetyltransferase immunoreactivity in these neurons. These results indicate that HGF may prevent the degeneration of motoneurons in adult humans with motoneuron injury and motor neuron diseases.



## 1. Introduction

Hepatocyte growth factor (HGF) was initially identified and purified as a potent mitogen of primary cultured hepatocytes (Nakamura et al., 1984, 1989). HGF is a heterodimeric protein composed of α and β chains and induces proliferation, migration, differentiation of target cells as well as organogenesis and neovascularization (Funakoshi and Nakamura, 2003). In the nervous system, HGF exhibits strong neurotrophic activities for motoneurons both in vitro and in vivo (Caton et al., 2000; Ebens et al., 1996; Funakoshi and Nakamura, 2003; Honda et al., 1995; Koyama et al., 2003, Maina and Klein, 1999; Naeem et al., 2002; Novak et al., 2000; Okura et al., 1999; Sun et al., 2002; Wong et al., 1997; Yamamoto et al., 1997). There have

* Corresponding author. Fax: +81 42 321 8678.
E-mail address: kazwtb@tmin.ac.jp (K. Watabe).

0006-8993/$ – see front matter © 2006 Elsevier B.V. All rights reserved.
doi:10.1016/j.brainres.2006.06.104

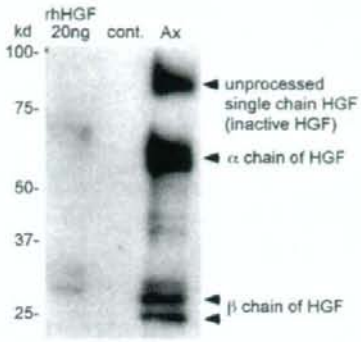


**Fig. 1 – Western blot analysis of conditioned media (CMs) obtained from COS1 cells uninfected (cont.) or infected (Ax) with AxCAhHGF. The CMs harvested at 3 days after infection were concentrated by heparin beads, electrophoresed, blotted and immunolabeled for HGF as described in the text.**

been no reports, however, concerning the neurotrophic effects of HGF on adult motoneuron death after proximal nerve injury. In animal models of adult motoneuron injury, avulsion of cranial and spinal nerves causes marked motoneuron degeneration in adult rats (Koliatsos et al., 1994; Moran and Graeber, 2004; Ruan et al., 1995; Sakamoto et al., 2000, 2003a, 2003b; Søreide, 1981; Watabe et al., 2000, 2005; Wu, 1993), so that these animal models can be useful for therapeutic evaluation of neurotrophic factors or neuroprotective molecules against adult motoneuron death (Ikeda et al., 2003; Sakamoto et al., 2000, 2003a, 2003b; Watabe et al., 2000, 2005). We have recently shown that adenoviral gene transfer of glial-cell-line-derived neurotrophic factor (GDNF), brain-derived neurotrophic factor (BDNF), transforming growth factor-β2 (TGFβ2) and growth inhibitory factor (GIF)/metallothionein-III (MT-III) prevented the death of adult rat facial and spinal motoneurons after facial nerve and cervical spinal root avulsion (Sakamoto et al., 2000, 2003a, 2003b; Watabe et al., 2000). In the present study, we investigated whether HGF protects injured motoneurons after facial nerve or spinal root avulsion by using a recombinant adenoviral vector encoding human HGF.

## 2. Results

### 2.1. *Bioassay of recombinant human HGF*

In this study, we constructed a recombinant adenoviral vector encoding human HGF (AxCAhHGF). To test the ability of AxCAhHGF to induce human HGF expression in vitro, COS1 cells were infected with AxCAhHGF and the conditioned media (CMs) were harvested at 3 days postinfection. The levels of human HGF in uninfected and infected CMs analyzed by enzyme-linked immunosorbent assay (ELISA) were 1.9± 0.4 ng/ml and 2004.8±160 ng/ml, respectively ($n=3$). Western blot analysis of the CM harvested at 3 days postinfection showed immunoreactive bands of α-chain, β-chain and pro-HGF (inactive, unprocessed single chain precursor form) (Fig. 1). The CM obtained from uninfected COS1 cells did not show any immunoreactive bands. The Madin-Darby canine kidney (MDCK) cell scatter assay showed definite bioactivitiy of AxCAhHGF-infected COS1 CM; i.e., the activity of 1:500-diluted CM containing 4 ng/ml HGF as measured by ELISA corresponded to that of 2 ng/ml recombinant human HGF (rhHGF) that induced scattering of MDCK cells (Fig. 2).

### 2.2. *Adenoviral-vector-mediated HGF gene expression in facial nuclei*

We then examined the expression of adenovirus-mediated HGF in injured motoneurons after avulsion. We have pre-

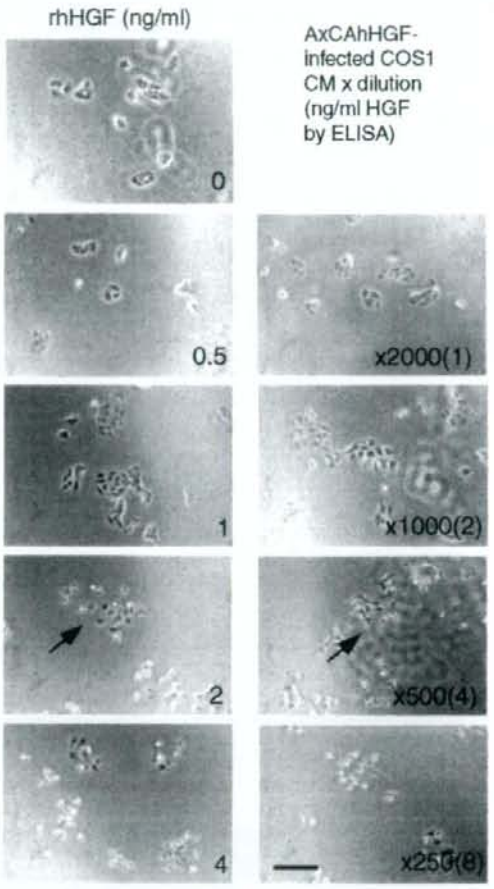


**Fig. 2 – Madin-Darby canine kidney (MDCK) cell scatter assay for HGF bioactivity. MDCK cells were cultured in the presence or absence of AxCAhHGF-infected COS1 CM or rhHGF as described in the text. The activity of 1:500-diluted CM containing 4 ng/ml human HGF as measured by ELISA corresponds to that of 2 ng/ml recombinant human HGF that induced scattering of MDCK cells (arrows). Scale bar=50 μm.**

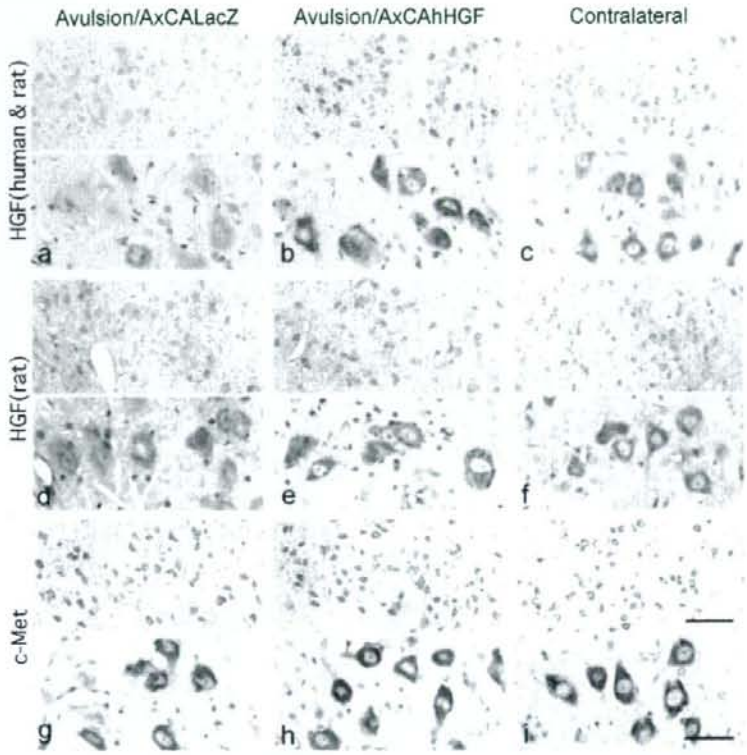


**Fig. 3 – Low (top) and high (bottom)-magnified photomicrographs of immunohistochemistry of facial motoneurons at the ipsilateral (a, b, d, e, g, h) and contralateral (c, f, i) sides 7 days after facial nerve avulsion and the treatment with AxCALacZ (a, d, g) or AxCAhHGF (b, c, e, f, h, i) using antibodies against human and rat HGF (a–c), rat HGF (b–f) and c-Met (g–i). Counterstained with hematoxylin. Injured facial motoneurons after avulsion and AxCAhHGF treatment are more intensely immunolabeled by anti-human and rat HGF antibody (b) compared with injured motoneurons with AxCALacZ treatment (a) or contralateral intact motoneurons (c). Immunoreactivity of injured motoneurons treated with AxCALacZ (d) or AxCAhHGF (e) is comparable to that of contralateral intact motoneurons (f) when anti-rat HGF antibody was used. Immunoreactivity for c-Met is consistently demonstrated in both injured and contralateral motoneurons (g–i). Scale bars = 200 μm (top), 50 μm (bottom).**

viously demonstrated that injured motoneurons and their axons were labeled with X-Gal after facial or seventh cervical segment (C7) avulsion and inoculation of an adenovirus encoding bacterial β-galactosidase gene as a reporter (AxCA-LacZ) into lesioned stylomastoid or vertebral foramen, respectively (Sakamoto et al., 2000; Watabe et al., 2000). This indicates the diffusion of the virus through the facial canal or intervertebral foramen, its adsorption to injured axons, retrograde transport of the virus via intramedullary facial or spinal nerve tracts to soma of the motoneurons and

**Table 1 – HGF protein levels in brain stem tissue containing facial nuclei after facial nerve avulsion and treatment with adenoviral vectors**

| Treatment ($n$ = animal number) | Human HGF (ng/g) | | Rat HGF (ng/g) | |
|---|---|---|---|---|
| | Ipsilateral | Contralateral | Ipsilateral | Contralateral |
| AxCALacZ ($n$ = 3) | u.d. | u.d. | 20.3 ± 3.8 | 17.2 ± 2.3 |
| AxCAhHGF ($n$ = 3) | 61.8 ± 36.1 | 13.1 ± 11.4 | 21.2 ± 3.1 | 22.8 ± 2.8 |

Seven days after facial nerve avulsion and the treatment with AxCALacZ or AxCAhHGF, the brain stem tissues containing facial nuclei (10–14 mg wet weight) were examined by human- and rat-specific HGF ELISA. u.d. = under the detection limit (<2.4 ng/g tissue).

successful induction of the virus-induced foreign gene in these neurons (Sakamoto et al., 2000, 2003a,b; Watabe et al., 2000). In the present study, 1 week after avulsion and treatment with AxCAhHGF, injured facial motoneurons were more intensely immunolabeled by an antibody that recognizes both human and rat HGF (Fig. 3b), compared with injured motoneurons treated with AxCALacZ (Fig. 3a) or uninjured motoneurons on the contralateral side (Fig. 3c). Immunoreactivity of injured motoneurons treated with AxCAhHGF (Fig. 3e), AxCALacZ (Fig. 3d) or phosphate-buffered saline (PBS) (not shown) was comparable to that of contralateral intact motoneurons (Fig. 3f) when an antibody that recognizes only rat HGF was used. These immunohistochemical results suggest that endogenous rat HGF was preserved in injured motoneurons after avulsion, while adenovirus-induced exogenous human HGF was successfully expressed in these neurons. Immunoreactivity for HGF receptor c-Met was consistently demonstrated in both ipsilateral and contralateral motoneurons after avulsion and AxCAhHGF or AxCALacZ treatment (Figs. 3g–i). No significant immunoreactivity for HGF and c-Met was observed in astrocytes, oligodendrocytes or microglia.

We further examined the expression of exogenous human HGF and endogenous rat HGF in brain stem tissue containing facial nuclei after facial nerve avulsion and adenovirus treatment by human-specific (Funakoshi and Nakamura, 2003) or rat-specific (Sun et al., 2002) ELISA (Table 1). Rat HGF levels measured by ELISA showed no significant difference between injured and contralateral sides. Human HGF levels were more than twofold compared with endogenous rat HGF levels after AxCAhHGF infection. Human HGF was also detectable in the tissues at the contralateral side after AxCAhHGF infection, which was considered to originate from injured and infected motoneurons at the ipsilateral side (Table 1).

One week after facial nerve avulsion and the treatment with AxCAhHGF, RT-PCR analysis showed that virus-induced human HGF mRNA transcripts were expressed in the brainstem tissue containing the facial nucleus on the ipsilateral, but not the contralateral side, whereas endogenous rat HGF

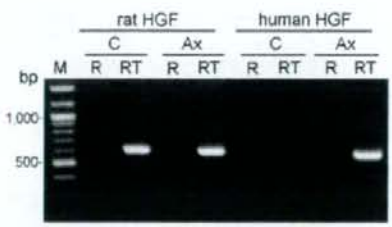


**Fig. 4 – RT-PCR analysis of HGF mRNA transcripts in ipsilateral (Ax) and contralateral (C) sides of the brain stem tissue containing facial nuclei 7 days after facial nerve avulsion and AxCAhHGF treatment. The PCRs were performed on RNA without (R) or with (RT) reverse transcription. Primers that amplify rat or human HGF mRNA transcripts were used as described in the text. M=DNA size marker.**


**Fig. 5 – Photomicrographs of facial motoneurons at the contralateral (a) and ipsilateral (b, c) side 4 weeks after the right facial nerve avulsion and the treatment of AxCALacZ (b) or AxCAhHGF (c). Pictures (a) and (c) were taken from the same section. Nissl stain. Scale bar=200 μm.**

mRNA was consistently detected in the tissues on both ipsilateral and contralateral sides after avulsion (Fig. 4).

### 2.3. *Neuroprotective effects of HGF gene transfer*

Four weeks after facial nerve or C7 spinal root avulsion and treatment with phosphate-buffered saline (PBS) or AxCALacZ, the number of surviving facial or spinal motoneurons declined to 30–50% of that on the contralateral side as described previously (Sakamoto et al., 2000, 2003a, 2003b; Watabe et al., 2000). The treatment with AxCAhHGF prevented the loss of facial (58.8±5.9% survival) and spinal (75.4±4.4% survival)

motoneurons after avulsion compared with the treatment with PBS (30.2±6.7% survival of facial motoneurons; 44.6±9.3% survival of C7 motoneurons) or AxCALacZ (32.4±4.3% survival of facial motoneurons; 46.0±5.3% survival of C7 motoneurons) (Sakamoto et al., 2000) (Figs. 5, 6; Table 2). The treatment with AxCAhHGF after avulsion attenuated the decrease of choline acetyltransferase (ChAT) immunoreactivity in injured facial motoneurons compared with the treatment with PBS or AxCALacZ (Fig. 7). We found no perivascular or intrathecal lymphocytic/mononuclear cell infiltration in the facial nuclei and the spinal cord tissues that would be histologically defined and identified in case of immunogenic reaction against adenovirus infection (Figs. 5, 6).

**Table 2 – Survival of motoneurons after facial nerve and spinal root avulsion and treatment with adenoviral vectors**

| Treatment ($n$=animal number) | Ipsilateral motoneuron number | Contralateral motoneuron number | % Survival |
|---|---|---|---|
| *Facial nerve avulsion* | | | |
| PBS ($n$=8) | 213±41 | 712±38 | 30.2±6.7 |
| AxCALacZ ($n$=4) | 239±29 | 741±73 | 32.4±4.3 |
| AxCAhHGF ($n$=7) | 441±87* | 745±38 | 58.8±5.9* |
| *Spinal root avulsion* | | | |
| PBS ($n$=4) | 66±22 | 144±20 | 44.6±9.3 |
| AxCALacZ ($n$=4) | 69±9 | 150±12 | 46.0±5.3 |
| AxCAhHGF ($n$=4) | 108±15** | 143±14 | 75.4±4.4** |

Numbers of facial motoneurons and the percent survival at the ipsilateral (lesion) side relative to the contralateral (control) side 4 weeks after avulsion and treatment with phosphate-buffered saline (PBS), AxCALacZ and AxCAhHGF. Results are presented as the mean±SD. Statistical comparison was done by Mann–Whitney U test. *$P<0.01$ vs. PBS- and AxCALacZ-treated groups. **$P<0.05$ vs. PBS- and AxCALacZ-treated groups.

## 3. Discussion

HGF binds to tyrosine kinase receptor c-Met and triggers diverse biological responses that include cell motility, proliferation, morphogenesis, neurite extension and anti-apoptotic activities in a variety of cells (Funakoshi and Nakamura, 2003; Maina and Klein, 1999). Although the function of HGF in the nervous system has not been fully elucidated, it has recently been shown that HGF plays a strong neuroprotective

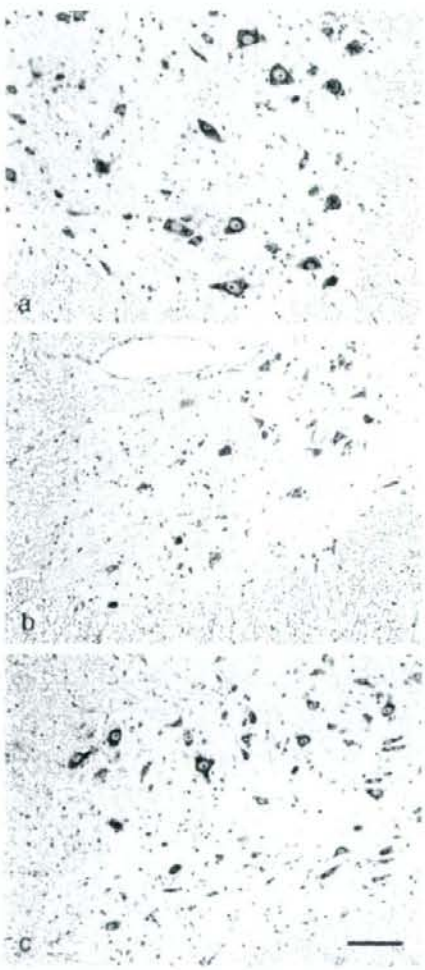


**Fig. 6 – Photomicrographs of C7 spinal motoneurons at the contralateral (a) and ipsilateral (b, c) side 4 weeks after the right C7 spinal nerve avulsion and the treatment of AxCALacZ (b) or AxCAhHGF (c). Pictures (a) and (c) were taken from the same section. Nissl stain. Scale bar=100 μm.**

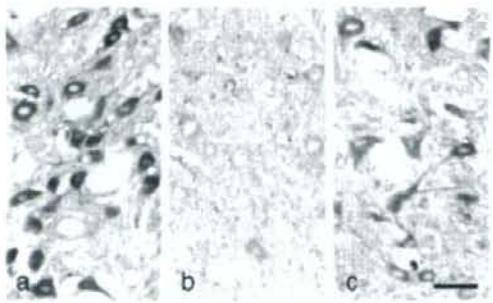


**Fig. 7 – Photomicrographs of ChAT immunohistochemistry (a–c) of facial motoneurons at the contralateral (a) and ipsilateral (b, c) side 7 days after the facial nerve avulsion and the treatment of AxCALacZ (b) or AxCAhHGF (c). Pictures (a) and (c) were taken from the same section. Scale bar=50 μm.**

role for motoneurons both in vitro and in vivo (Caton et al., 2000; Ebens et al., 1996; Honda et al., 1995; Koyama et al., 2003; Naeem et al., 2002; Novak et al., 2000; Okura et al., 1999; Sun et al., 2002; Wong et al., 1997; Yamamoto et al., 1997). It has been demonstrated that HGF-c-Met receptor coupling leads anti-apoptotic activities via MAP kinase (Hamanoue et al., 1996) and phosphatidylinositol-3 kinase/Akt (Hossain et al., 2002; Zhang et al., 2000) pathways and prevents caspase-1 and inducible nitric oxide synthase induction in motoneurons (Sun et al., 2002). In addition, HGF up-regulates the expression of excitatory amino acid transporter 2/glutamate transporter 1 (EAAT2/GLT1) in primary cultured astrocytes, which may improve glutamate clearance and reduce glutamate-mediated neurotoxicity (Sun et al., 2002).

In the present study, we investigated whether the treatment of AxCAhHGF can prevent the degeneration of motoneurons in adult rats after facial nerve and spinal root avulsion. We produced AxCAhHGF that induced bioactive HGF protein in infected COS1 cells in vitro as demonstrated by ELISA, Western blot analysis and MDCK scatter assay. Immunohistochemistry and RT-PCR results indicated that AxCAhHGF successfully infected injured motoneurons after facial nerve avulsion, suggesting the autocrine and paracrine neurotrophic effects of exogenous HGF on injured motoneurons after avulsion. Subsequently, we demonstrated that the treatment of AxCAhHGF delayed the loss of injured facial and spinal motoneurons. In addition, peripheral nerve avulsion as well as axotomy induces rapid decrease of ChAT immunoreactivity in injured motoneurons (Sakamoto et al., 2000; Watabe et al., 2000). In the present study, AxCAhHGF treatment after facial nerve avulsion improved ChAT immunoreactivity in injured motoneurons. We have previously shown that the treatments of recombinant adenoviral vectors encoding GDNF, BDNF, TGFβ2 and GIF promote the survival of motoneurons and attenuated ChAT immunoreactivity in the same avulsion model (Sakamoto et al., 2000, 2003a, 2003b; Watabe et al., 2000). Similarly, the present results clearly indicate that HGF have neuroprotective effects on injured adult motoneurons.

It has been reported that HGF mRNA is up-regulated in the spinal cord of human sporadic amyotrophic lateral sclerosis (ALS) (Jiang et al., 2005), and certain residual anterior horn cells in the spinal cord of ALS patients co-express both HGF and c-Met with the same or even stronger intensity compared with those of normal subjects (Kato et al., 2003). Transgenic mice expressing human mutant Cu/Zn superoxide dismutase (G93A mice) overexpressing HGF exhibited significant prolongation in survival and decreased motoneuron death compared with G93A mice with normal HGF expression (Sun et al., 2002). These reports indicate that HGF may have protective effects on motoneuron degeneration in ALS. Together with the present data, it is therefore conceivable that HGF may prevent the degeneration of motoneurons in adult patients with motoneuron injury and motor neuron diseases such as ALS.

In conclusion, we examined neuroprotective effects of HGF on injured adult motoneurons. The treatment of an adenoviral vector encoding HGF after facial nerve and spinal root avulsion significantly improved the survival of injured facial and spinal motoneurons and ameliorated ChAT immunoreactivity in these neurons. These results indicate that HGF may be a potential neuroprotective agent against motoneuron injury and motor neuron diseases in adult humans.

## 4. Experimental procedures

### 4.1. *Adenovirus preparation*

The human HGF cDNA was excised from pBS-hHGF with deletion of 15 base pairs (Seki et al., 1990) and subsequently cloned into *Swa*I cloning site of a cassette cosmid pAxCAwt (TaKaRa, Osaka, Japan) carrying an adenovirus type-5 genome lacking the E3, E1A and E1B regions to prevent the virus replication. The cosmid pAxCAwt contains the CAG (cytomegalovirus-enhancer-chicken β-actin hybrid) promoter on the 5′ end and a rabbit globin poly (A) sequence on the 3′ end. The cosmid was then cotransfected to 293 cells with the adenovirus genome lacking the E3 region (Miyake et al., 1996). A recombinant adenoviral vector encoding HGF (AxCAhHGF) was propagated and isolated from 293 cells and purified by two rounds of CsCl centrifugation. Generation of recombinant adenovirus containing bacterial β-galactosidase gene (AxCA-LacZ) has been described elsewhere (Kanegae et al., 1996).

### 4.2. *Analysis of HGF expression in COS1 cells infected with AxCAhHGF*

COS1 cells were infected with AxCAhHGF at a multiplicity of infection (moi) of 100 in serum-free Dulbecco's minimum essential medium (DMEM) (Invitrogen, Carlsbad, CA) for 1 h and incubated with serum-free DMEM in 5% $CO_2$ at 37 °C. The conditioned media (CMs) were harvested at 3 days postinfection for ELISA and Western blot analysis. The ELISA was performed as described (Sun et al., 2002; Funakoshi and Nakamura, 2003). For Western blot analysis, CM was treated with heparin beads to concentrate HGF and the CM or rhHGF (Nakamura et al., 1989; Seki et al., 1990) was electrophoresed on 4–20% gradient sodium dodecyl sulfate (SDS)/polyacrylamide gels under reduced condition and transferred to PVDF membrane (Atto, Tokyo, Japan). The blotted membrane was then blocked with 3% skim milk and incubated overnight with rabbit anti-HGF (1:500; Tokusyu Meneki, Tokyo, Japan) followed by incubation with goat anti-rabbit IgG–HRP conjugate (1:1,000; DAKO, Glostrup, Denmark). Reactions were visualized by enhanced chemiluminescence detection using an ECL Western blotting detection kit (Amersham, Piscataway, NJ).

### 4.3. *Bioassay of adenoviral HGF; MDCK scatter assay*

MDCK cells cultured in DMEM with 10% fetal bovine serum (FBS) were trypsinized, seeded on 24-well plate (5000 cells/well) in the presence or absence of AxCAhHGF-infected COS1 CMs or rhHGF in DMEM with 5% FBS and incubated for 24 h at 37 °C. The cell scattering was viewed under a phase contrast microscope.

### 4.4. *Animals and surgical procedures*

The experimental protocols were approved by the Animal Care and Use Committee of the Tokyo Metropolitan Institute for Neuroscience.

#### 4.4.1. *Facial nerve avulsion*

Adult Fischer 344 male rats (12–14 weeks old, 200–250 g) were anesthetized with intraperitoneal injection of pentobarbital sodium (40 mg/kg). Under a dissecting microscope, the right facial nerve was exposed at its exit from the stylomastoid foramen. Using microhemostat forceps, the proximal facial nerve was avulsed by gentle traction and removed from the distal facial nerve as described previously (Sakamoto et al., 2000). Immediately following the avulsion, microsyringe was inserted into the stylomastoid foramen and 20 μl solution of AxCAhHGF ($1\times10^8$ pfu), AxCALacZ ($1\times10^8$ pfu) or PBS was injected through the facial canal. The wounds were covered with a small piece of gelatin sponge (Gelfoam; Pharmacia Upjohn, Bridgewater, NJ) and suture closed, and the animals were sacrificed at 1 and 4 weeks postoperation as described below.

#### 4.4.2. *Spinal root avulsion*

Anesthetized animals were placed in a supine position. Under a dissecting microscope, the right seventh cervical segment (C7) nerve was exposed by separating the surrounding cervical muscles and connective tissue until the point where the vertebral foramen was identified. Using microhemostat forceps, the C7 ventral and dorsal roots and dorsal root ganglia (DRG) were avulsed and removed from the peripheral nerve as described previously (Watabe et al., 2000). Immediately following avulsion, a small piece of Gelfoam presoaked with 10 μl solution of AxCAhHGF ($1\times10^8$ pfu), AxCALacZ ($1\times10^8$ pfu) or PBS was placed in contact with the lesioned vertebral foramen. The wounds were suture closed and animals were sacrificed at 4 weeks postoperation as described below.

### 4.5. *HGF ELISA of brain stem tissue containing facial nucleus*

One week after facial nerve avulsion and the treatment with AxCALacZ or AxCAhHGF, the animals ($n=3$) were euthanized with a lethal dose of pentobarbital sodium and the brain stem tissue containing the facial nucleus (11–14 mg wet weight) was collected. ELISA for rat HGF and human HGF was performed as described (Sun et al., 2002; Funakoshi and Nakamura, 2003).

### 4.6. *Reverse transcription followed by polymerase chain reaction (RT-PCR)*

One week after facial nerve avulsion and the treatment with AxCAhHGF, the brain stem tissue containing the facial nucleus ($n=3$) was collected as described above. Total RNA was isolated from the tissue using RNA isolation reagent (TRIZOL, Invitrogen, Carlsbad, CA) according to the manufacturer's instructions and treated with RNase-free DNase (Roche, Penzberg, Germany) in transcription buffer for 30 min. First strand cDNA was synthesized from 250 ng of total RNA using random primer and Superscript II reverse transcriptase (Invitrogen) for one PCR analysis. The PCR reactions were carried out in PCR buffer containing cDNA template, 200 μM dNTPs, 2 mM $MgCl_2$, 0.2 μM of each primer and 25 unit/ml of ExTaq DNA polymerase (TaKaRa, Osaka, Japan). Specific oligonucleotide primers for PCR were designed to amplify rat HGF cDNA (Tashiro et al., 1990; GenBank Accession no. NM_017017; forward, 5′-GCCAAAACAAAA-CAACTG-3′; reverse, 5′-GACACCAAGAACCATTCTCA-3′) that yield 615 bp amplified products, and human HGF cDNA (Seki et al., 1990; M60718; forward, 5′-AAACATATCTGCGGAGGATC-3′; reverse, 5′-ACGATTTGGAATGGCACATC-3′) that give 561 bp amplified products. The PCR amplification program consisted of denaturation at 95 °C for 1 min, annealing at 55 °C for 1 min and extension at 72 °C for 1 min for 40 cycles. For negative control reactions, non-reverse transcribed RNA samples were processed for PCR to exclude the possibility of the contamination of genomic or adenoviral DNA as a source of amplified products. The PCR products were subjected to electrophoresis on a 1.5% agarose gel stained with ethidium bromide. To confirm the sequence identity of the amplified products, the PCR fragments were subcloned into pCRII (Invitrogen) and sequenced by a model 373A sequencer and the ABI PRISM BigDye Terminator Cycle Sequencing Kit (Applied Biosystems, Foster City, CA).

### 4.7. *Histological analysis*

Rats were anesthetized with a lethal dose of pentobarbital sodium and transcardially perfused with 0.1 M phosphate buffer, pH 7.4 (PB) followed by 4% paraformaldehyde in 0.1 M PB. The brain stem tissue containing facial nuclei and their intramedullary nerve tracts after facial nerve avulsion or the C7 spinal cord tissue after spinal root avulsion was dissected and immersion fixed in the same fixative for 2 h. As for facial nerve avulsion, we routinely checked the absence of extra-axial portion of facial nerve on the avulsed side under a dissecting microscope and confirmed the absence of any peripheral nerve tissues at the level of facial nerve outlet from the brain stem in microscopic sections prepared from every animal as described below. As for C7 spinal root avulsion, the absence of C7 ventral and dorsal roots as well as DRG on the lesioned side was confirmed under the dissecting microscope. A small longitudinal incision was made in the anterolateral white matter through the level of C7 ventral root outlets on the contralateral side in aid of identifying the level of C7 spinal ventral horn in histological sections.

For immunohistochemistry, the brain stem tissues were either embedded in paraffin or cryoprotected in 30% sucrose in 0.1 M PB and serial paraffin or cryostat sections were made. For immunostaining for HGF, deparaffinized sections were pretreated with 0.3% $H_2O_2$ in methanol, incubated with 0.05% trypsin for 15 min at 37 °C and preincubated with 3% heat-inactivated goat serum in 0.1% Triton-X100 in phosphate-buffered saline (T-PBS). Sections were then incubated overnight at 4 °C with rabbit anti-human HGFα antibody (H55; recognizes human and rat HGFα; IBL, Fujioka, Japan) or rat HGFα antibody (H56; recognizes rat, but not human, HGFα; IBL) diluted 1:200 in T-PBS followed by the incubation with biotinylated goat anti-rabbit IgG at a dilution of 1:200 and with ABC reagent (Vector). Immunostaining for ChAT on cryostat sections was performed using rabbit polyclonal antibody to ChAT (1:1000; Chemicon, Temecula, CA) and ABC method as described previously (Watabe et al., 2000). Sections were visualized by 3,3′-diaminobenzidine tetrahydrocholoride (DAB)–$H_2O_2$ solution and counterstained with hematoxylin.

For negative controls, the primary antibodies were omitted or replaced by non-immunized animal sera.

For motoneuron cell counting, serial paraffin-embedded brain stem or C7 spinal cord sections were made. Every fifth section (6 μm thickness; 24 μm interval) was picked up, deparaffinized and stained with cresyl violet (Nissl staining). Facial motoneurons having nuclei containing distinct nucleoli on both sides of the facial nuclei were counted in 25 sections. For spinal motoneuron cell counting, ventral horn motoneurons located in Rexed's lamina IX having nuclei greater than 15 μm in diameter with distinct nucleoli on both sides of the C7 spinal cord were counted in 35 sections. The data were then expressed as the mean ± SD from 4 to 8 animals, and statistical significance was assessed by Mann–Whitney *U* test.

## Acknowledgments

We are grateful to Dr. Jing-Song Shen (Jikei University School of Medicine) for adenovirus preparation. This work was supported by Grants-in-Aid for Ministry of Education, Culture, Sports, Science and Technology, Japan, and Research on Psychiatric and Neurological Diseases and Mental Health, H16-kokoro-017, Ministry of Health, Labor and Welfare, Japan.

## REFERENCES

Caton, A., Hacker, A., Naeem, A., Livet, J., Maina, F., Bladt, F., Klein, R., Birchmeier, C., Guthrie, S., 2000. The branchial arches and HGF are growth-promoting and chemoattractant for cranial motor axons. Development 127, 1751–1766.

Ebens, A., Brose, K., Leonardo, E.D., Hanson Jr., M.G., Bladt, F., Birchmeier, C., Barres, B.A., Tessier-Lavigne, M., 1996. Hepatocyte growth factor/scatter factor is an axonal chemoattractant and a neurotrophic factor for spinal motor neurons. Neuron 17, 1157–1172.

Funakoshi, H., Nakamura, T., 2003. Hepatocyte growth factor: from diagnosis to clinical applications. Clin. Chim. Acta 327, 1–23.

Hamanoue, M., Takemoto, N., Matsumoto, K., Nakamura, T., Nakajima, K., Kohsaka, S., 1996. Neurotrophic effect of hepatocyte growth factor on central nervous system neurons in vitro. J. Neurosci. Res. 43, 554–564.

Honda, S., Kagoshima, M., Wanaka, A., Tohyama, M., Matsumoto, K., Nakamura, T., 1995. Localization and functional coupling of HGF and c-Met/HGF receptor in rat brain: implication as neurotrophic factor. Brain Res. Mol. Brain Res. 32, 197–210.

Hossain, M.A., Russell, J.C., Gomez, R., Laterra, J., 2002. Neuroprotection by scatter factor/hepatocyte growth factor and FGF-1 in cerebellar granule neurons is phosphatidylinositol 3-kinase/akt-dependent and MAPK/CREB-independent. J. Neurochem. 81, 365–378.

Ikeda, K., Sakamoto, T., Marubuchi, S., Kawazoe, Y., Terashima, N., Iwasaki, Y., Kinoshita, M., Ono, S., Nakagawa, M., Watabe, K., 2003. Oral administration of a neuroprotective compound T-588 prevents motoneuron degeneration after facial nerve avulsion in adult rats. Amyotroph. Lateral. Scler. Other Mot. Neuron Disord. 4, 74–80.

Jiang, Y.M., Yamamoto, M., Kobayashi, Y., Yoshihara, T., Liang, Y., Terao, S., Takeuchi, H., Ishigaki, S., Katsuno, M., Adachi, H., Niwa, J., Tanaka, F., Doyu, M., Yoshida, M., Hashizume, Y., Sobue, G., 2005. Gene expression profile of spinal motor neurons in sporadic amyotrophic lateral sclerosis. Ann. Neurol. 57, 236–251.

Kanegae, Y., Takamori, K., Sato, Y., Lee, G., Nakai, M., Saito, I., 1996. Efficient gene activation system on mammalian cell chromosomes using recombinant adenovirus producing Cre recombinase. Gene 181, 207–212.

Kato, S., Funakoshi, H., Nakamura, T., Kato, M., Nakano, I., Hirano, A., Ohama, E., 2003. Expression of hepatocyte growth factor and c-Met in the anterior horn cells of the spinal cord in the patients with amyotrophic lateral sclerosis (ALS): immunohistochemical studies on sporadic ALS and familial ALS with superoxide dismutase 1 gene mutation. Acta Neuropathol. (Berl.) 106, 112–120.

Koliatsos, V.E., Price, W.L., Pardo, C.A., Price, D.L., 1994. Ventral root avulsion: an experimental model of death of adult motor neurons. J. Comp. Neurol. 342, 35–44.

Koyama, J., Yokouchi, K., Fukushima, N., Kawagishi, K., Higashiyama, F., Moriizumi, T., 2003. Neurotrophic effect of hepatocyte growth factor on neonatal facial motor neurons. Neurol. Res. 25, 701–707.

Maina, F., Klein, R., 1999. Hepatocyte growth factor, a versatile signal for developing neurons. Nat. Neurosci. 2, 213–217.

Miyake, S., Makimura, M., Kanegae, Y., Harada, S., Sato, Y., Takamori, K., Tokuda, C., Saito, I., 1996. Efficient generation of recombinant adenoviruses using adenovirus DNA-terminal protein complex and a cosmid bearing the full-length virus genome. Proc. Natl. Acad. Sci. U. S. A. 93, 1320–1324.

Moran, L.B., Graeber, M.B., 2004. The facial nerve axotomy model. Brain Res. Brain Res. Rev. 44, 154–178.

Naeem, A., Abbas, L., Guthrie, S., 2002. Comparison of the effects of HGF, BDNF, CT-1, CNTF, and the branchial arches on the growth of embryonic cranial motor neurons. J. Neurobiol. 51, 101–114.

Nakamura, T., Nawa, K., Ichihara, A., 1984. Partial purification and characterization of hepatocyte growth factor from serum of hepatectomized rats. Biochem. Biophys. Res. Commun. 122, 1450–1459.

Nakamura, T., Nishizawa, T., Hagiya, M., Seki, T., Shimonishi, M., Sugimura, A., Tashiro, K., Shimizu, S., 1989. Molecular cloning and expression of human hepatocyte growth factor. Nature 342, 440–443.

Novak, K.D., Prevette, D., Wang, S., Gould, T.W., Oppenheim, R.W., 2000. Hepatocyte growth factor/scatter factor is a neurotrophic survival factor for lumbar but not for other somatic motoneurons in the chick embryo. J. Neurosci. 20, 326–337.

Okura, Y., Arimoto, H., Tanuma, N., Matsumoto, K., Nakamura, T., Yamashima, T., Miyazawa, T., Matsumoto, Y., 1999. Analysis of neurotrophic effects of hepatocyte growth factor in the adult hypoglossal nerve axotomy model. Eur. J. Neurosci. 11, 4139–4144.

Ruan, R.S., Leong, S.K., Yeoh, K.H., 1995. The role of nitric oxide in facial motoneuronal death. Brain Res. 698, 163–168.

Sakamoto, T., Watabe, K., Ohashi, T., Kawazoe, Y., Oyanagi, K., Inoue, K., Eto, Y., 2000. Adenoviral vector-mediated GDNF gene transfer prevents death of adult facial motoneurons. NeuroReport 11, 1857–1860.

Sakamoto, T., Kawazoe, Y., Shen, J.S., Takeda, Y., Arakawa, Y., Ogawa, J., Oyanagi, K., Ohashi, T., Watanabe, K., Inoue, K., Eto, Y., Watabe, K., 2003a. Adenoviral gene transfer of GDNF, BDNF and TGF beta 2, but not CNTF, cardiotrophin-1 or IGF1, protects injured adult motoneurons after facial nerve avulsion. J. Neurosci. Res. 72, 54–64.

Sakamoto, T., Kawazoe, Y., Uchida, Y., Hozumi, I., Inuzuka, T., Watabe, K., 2003b. Growth inhibitory factor prevents degeneration of injured adult rat motoneurons. NeuroReport 14, 2147–2151.

Seki, T., Ihara, I., Sugimura, A., Shimonishi, M., Nishizawa, T., Asami, O., Hagiya, M., Nakamura, T., Shimizu, S., 1990. Isolation and expression of cDNA for different forms of hepatocyte growth factor from human leukocyte. Biochem. Biophys. Res. Commun. 172, 321–327.